Acta Crystallographica Section B
Structural Science
ISSN 0108-7681

Structure of ν-$Al_{80.61}Cr_{10.71}Fe_{8.68}$, a giant hexagonal approximant of a quasicrystal determined by a combination of electron microscopy and X-ray diffraction

Z. M. Mo,[a,b] H. Y. Zhou[c] and K. H. Kuo[a,b]*

[a]Beijing Laboratory of Electron Microscopy, Institute of Physics, Chinese Academy of Sciences, PO Box 2724, Beijing 100080, People's Republic of China, [b]Department of Materials Engineering, Dalian University of Technology, Dalian 116023, People's Republic of China, and [c]X-ray Laboratory, Center for Analysis, China University of Geosciences, Wuhan 430074, People's Republic of China

Correspondence e-mail: khkuo@yahoo.com

Received 25 August 1999
Accepted 6 December 1999

ν-$Al_{80.61}Cr_{10.71}Fe_{8.68}$, $P6_3/m$ (No. 176), a = 40.68 (7), c = 12.546 (1) Å, V = 17 983 (8) Å^3, atoms/cell = 1184.56, D_x = 3.518 g cm^{-3}, λ(Mo $K\alpha$) = 0.71069 Å, μ = 5.032 mm^{-1}, $F(000)$ = 18 433, T = 293 K, final R = 0.075 for 3854 reflections with $F_o > 4\sigma(F_o)$. The [001] high-resolution electron-microscopic image of the ν-AlCrFe phase clearly shows similar local characteristics to those given by the complex icosahedral cluster found in somewhat smaller hexagonal approximant structures, such as κ-$Al_{76}Cr_{18}Ni_6$ [a = 17.674 (3), c = 12.516 (3) Å; Sato *et al.* (1997). *Acta Cryst.* C**53**, 1531–1533; Marsh (1998). *Acta Cryst.* B**54**, 925–926] and λ-$Al_{4.32}Mn$ [a = 28.382 (9), c = 12.389 (2) Å; Kreiner & Franzen (1997). *J. Alloys Compd.* **261**, 83–104]. Using the known atomic distribution of this icosahedral cluster in the κ and λ phases as the starting point, the structure of the ν phase, a hexagonal intermetallic compound with probably the largest a parameter, was solved by X-ray single-crystal diffraction using direct methods. As in κ and λ phases, almost all TM (transition metal) atoms in the complex icosahedral cluster are icosahedrally coordinated. However, contrary to the λ structure in which about 98% of the TM atoms have icosahedral coordination, the TM atoms in the ν structure also form capped pentagonal prisms in the region between these complex icosahedral clusters, yielding an average icosahedral coordination of about 70% for TM atoms. After rapid solidification, the ν phase occurs together with a decagonal quasicrystal with a periodicity of about 12.5 Å along its tenfold axis and thus also consists of six layers, two flat ones each sandwiched between two puckered layers in mirror reflection, stacked along the c axis.

1. Introduction

After the discovery of the icosahedral quasicrystal in very rapidly solidified $Al_{86}Mn_{14}$ and Al–Mn–Si alloys, the hexagonal phases μ-Al_4Mn, λ-Al_4Mn and β-Al_9Mn_3Si (isostructural to φ-$Al_{10}Mn_3$) have been found to coexist with this quasicrystal (Audier & Guyot, 1986; Bendersky, 1987*a*,*b*; Dubois *et al.*, 1988). The structure of the hexagonal β-Al_9Mn_3Si phase was determined by Robinson (1952), while the icosahedral cluster in it was analyzed by Kripjakevich (1977). However, the structures of the μ-Al_4Mn and λ-Al_4Mn phases were determined only recently (Table 1). Almost all Mn atoms are located at the centers of slightly distorted icosahedra propagated in the $\langle uv0\rangle$ directions to form an icosahedral (001) layer block (Shoemaker *et al.*, 1989; Franzen & Kreiner, 1993; Shoemaker, 1993; Kreiner & Franzen, 1997). This (001) icosahedral layer block is about 4 Å thick, so that the c parameter of the hexagonal phase is a multiple of 4 Å,

Table 1
Some hexagonal approximants of quasicrystals.

Phase	Space group	a (Å)	c (Å)	Literature
κ-$Al_{76}Cr_{18}Ni_6$†	$P6_3$	17.674	12.516	Sato *et al.* (1997)
	$P6_3/m$			Marsh (1998)
λ-Al_4Mn	$P6_3/m$	28.382	12.389	Franzen & Kreiner (1993)
				Kreiner & Franzen (1997)
ν-$Al_{80.61}Cr_{10.71}Fe_{8.68}$	$P6_3/m$	40.0	12.4	Sui *et al.* (1999)
		40.687	12.546	Present work
Al_5Co_2	$P6_3/mmc$	7.671	7.608	Bradley & Cheng (1938)
β-Al_9Mn_3Si	$P6_3/mmc$	7.500	7.772	Robinson (1952)
φ-$Al_{10}Mn_3$	$P6_3/mmc$	7.543	7.898	Taylor (1959)
μ-Al_4Mn‡	$P6_3/mmc$	19.98	24.673	Shoemaker *et al.* (1989)
C14-$MgZn_2$(μ_1)	$P6_3/mmc$	5.15	8.48	Friauf (1927)
S-$Zn_{65.22}Mg_{27.92}Y_{6.86}$	$P6_3/mmc$	14.579	8.687	Takakura *et al.* (1998)
μ_3-$Zn_{65.2}Mg_{28.3}Sm_{6.5}$	$P6_3/mmc$	14.619	8.708	Sugiyama *et al.* (1998)
μ_3-$Zn_{63.8}Mg_{28.6}Gd_{7.7}$	$P6_3/mmc$	14.633	8.761	Sugiyama *et al.* (1998)
M-Zn_6Mg_3Sm	$P6_3/mmc$	23.5	8.6	Abe *et al.* (1999)
μ_7-$Zn_{64.8}Mg_{24.1}Sm_{11.1}$	$P6_3/mmc$	33.565	8.873	Sugiyama *et al.* (1999)

† It should be pointed out that a family of intermetallic phases with φ-$Al_{10}Mn_3$ as the basic structure was also called κ phases (Hårsta & Runqvist, 1987). This should not be mixed with the κ-$Al_{76}Cr_{18}Ni_6$ discussed in the present work (Sato *et al.*, 1997). ‡ The μ_3 and μ_7 Zn–Mg–Sm superstructures (Sugiyama *et al.*, 1998, 1999) are related to the Friauf–Laves $MgZn_2$ (μ_1) phase and have nothing to do with μ-Al_4Mn.

about the same as the periodicity along the tenfold axis of the two-dimensional decagonal quasicrystal co-existing with it (Li & Kuo, 1988). Such a crystalline phase with a composition and local structure similar to a quasicrystal is called a crystalline approximant or simply an approximant of a quasicrystal (Elser & Henley, 1985). Obviously, a study of the structure of the crystalline approximant and the complex icosahedral cluster in it might shed some light on elucidating the structure of a quasicrystal.

Recently, another two hexagonal phases akin to λ-Al_4Mn have been found: one is κ-$Al_{76}Cr_{18}Ni_6$ (Sato *et al.*, 1997; Marsh, 1998) and the other is ν-$Al_{80.61}Cr_{10.71}Fe_{8.68}$, to be discussed in the present paper. The latter hexagonal phase was found recently by Sui *et al.* (1999) and was called the H-AlFeCr phase in order to differentiate it from the orthorhombic O-AlFeCr phase (Sui *et al.*, 1997) and the monoclinic M-AlFeCr phase (Liao *et al.*, 1998) found in the same $Al_{12}Fe_2Cr$ alloy. The close structural relationship between the κ-$Al_{76}Cr_{18}Ni_6$ and λ-Al_4Mn phases has been pointed out earlier (Li *et al.*, 1997). Quite recently, the similarity in the [001] electron diffraction patterns of the κ, λ and ν phases as well as the similarity in the [001] high-resolution electron microscopic (HREM) images of the κ and ν phases have been discussed by Sui *et al.* (1999). It is to be noted from Table 1 that the hexagonal κ, λ and ν phases have about the same c parameter (12.4–12.6 Å) and, after rapid solidification, all these phases occur together with a decagonal quasicrystal.

In the present investigation the HREM image with a resolution of about 2 Å taken along the [001] axis of the ν phase showed almost the same local characteristics around a lattice point as the complex icosahedral cluster in the κ-AlCrNi phase reported by Li *et al.* (1997). Furthermore, a κ-AlCrFe phase occurred side by side with the ν-AlCrFe phase in the $Al_{12}Cr_2Fe$ alloy and the strong diffraction spots in the approximate [250] electron diffraction pattern of both the κ and ν phases showed a pseudo-fivefold distribution analogous to the fivefold electron diffraction pattern of a quasicrystal. As mentioned above, the structures of κ and λ are closely related (Li *et al.*, 1997). These gave the clue that the κ, λ and ν structures might consist of similar complex icosahedral clusters. Using the complex icosahedral cluster based on the data given for κ by Marsh (1998) and for λ by Kreiner & Franzen (1997) as a starting point, the structure of the ν phase was solved by X-ray single-crystal diffraction using direct methods. According to the *Atlas of Crystal Structure Types for Intermetallic Phases* (Daams *et al.*, 1991), the structure of the ν phase is probably the hexagonal intermetallic structure with the largest a parameter ever solved. Its unit-cell content (about 1184 atoms) is comparable to that of the giant cubic intermetallic compounds with complicated icosahedral networks studied by Samson ($NaCd_2$, 1192 atoms; β-Mg_2Al_3, 1168 atoms; Cu_4Cd_3, 1116 atoms; for a review, see Samson, 1987), while the number of unique sites is much larger.

2. Experimental

An Al–Cr–Fe alloy with a nominal composition of $Al_{12}Cr_2Fe$ was prepared by melting a mixture of high-purity Al (99.9999 wt%), Cr (99.9 wt%) and Fe (99.5 wt%) in an oven and cooled in a sand bath. Thin films for electron microscopy were made from the bulk sample by slicing, grinding and ion milling. HREM images were taken with a Jeol 2010 electron microscope working at 200 kV with an interpretable resolution of 2 Å. Simulated HREM images were calculated (aperture 0.531 $Å^{-1}$, spherical aberration 0.5 mm) using the commercial *CERIUS*^{2} package (Molecular Simulations Inc., MA, USA).

A hexagonal needle-like single crystal with the dimensions 0.1 × 0.12 × 0.6 mm was selected in the cavities of the cast ingot after checking its quality by procession photographs. Its chemical composition, $Al_{81}Cr_{11}Fe_8$, was determined by electron microprobe analysis. The intensity data were collected on a Rigaku AFC5R four-circle diffractometer with graphite-monochromated Mo $K\alpha$ radiation. The ω–2θ scan technique was used, scan rate 8.0° min^{-1}, scan width $(1.35 + 0.35 \tan\theta)°$. The lattice parameters were refined with 23 reflections in the 18–47° 2θ range. The ratio of peak counting time to background counting time was 2:1. Three standard reflections had an average intensity variation of 0.6%. The space group was found to be $P6_3/m$ (No. 176) in a previous transmission electron microscopic study (Sui *et al.*, 1999) and data were

collected in the range $0 \leq h, k \leq 50, 0 \leq l \leq 15$. The absorption correction was performed by means of a ψ-scan algorithm and the transmission factors ranged between 0.481 and 0.593. Owing to the poor crystallinity of the single crystal, only 5453 unique reflections with $F_o > 1.5\sigma(F_o)$ were retained and structure determination was based on these reflections.[1]

3. Structure determination

A straightforward application of direct methods intending to yield a plausible structural model of the ν phase was unsuccessful. This was not unexpected since similar attempts to solve the hexagonal μ-Al_4Mn (Shoemaker *et al.*, 1989) and λ-Al_4Mn (Kreiner & Franzen, 1997) phases with about half the atoms per unit cell as ν were also unsuccessful. Rather than using the Patterson method to solve these structures as these authors did, the present authors relied on a combination of transmission electron microscopy and X-ray single-crystal diffraction to solve the structure of the hexagonal ν phase.

3.1. Transmission electron microscopy

Experimental HREM images were taken along the [001] axis of the ν phase with different focus values of the objective lens. The image taken at the Scherzer defocus value of −480 Å gives the best resolution. After taking due consideration of the electron optical parameters of the objective lens, this image, according to the weak-phase-object approximation, corresponds to the projected [001] structure of the ν phase. However, the contrast of this image is very poor. In order for a comparison to be made with the [001] HREM images of the κ and λ phases with good contrast, a [001] HREM image of the ν phase was taken at a defocus value of about −640 Å. Using the *CRISP* program of Hovmöller (1992), the raw [001] HREM image was Fourier transformed, filtered and averaged with due consideration to its $P6_3/m$ space group to reduce the noise background, and then inversely Fourier transformed to yield the filtered image (Fig. 1*c*). The plane cell of the ν phase is marked with large solid circles. There are two main features to be noted in this HREM image. First, there is a hexagonal set of small image points around each lattice point and the six corners of it are marked with asterisks. Second, the image points in this hexagon form a set of sixfold clockwise curved spokes. It is of interest to note that the [001] HREM image of the κ-AlCrNi phase, reported in Fig. 8(*b*) of Li *et al.* (1997), also consists of the same hexagonal set of image points. For comparison, the simulated [001] HREM images of both the κ and λ phases, shown in Figs. 1(*a*) and 1(*b*), were calculated for a thickness of 100 Å and a defocus value of −640 Å using the atomic sites given by Marsh (1998) and Kreiner & Franzen (1997), respectively. Comparing the image points in the hexagons in Figs. 1(*a*), 1(*b*) and 1(*c*), it is obvious that the hexagons in them have the same size and content, although the orientation of these hexagons is slightly different. Moreover, the sixfold clockwise curved distribution of image points inside these hexagons is also the same. These provide strong evidence to support the assumption that a complex icosahedral cluster similar to that existing in the κ and λ phases may also exist in the ν phase.

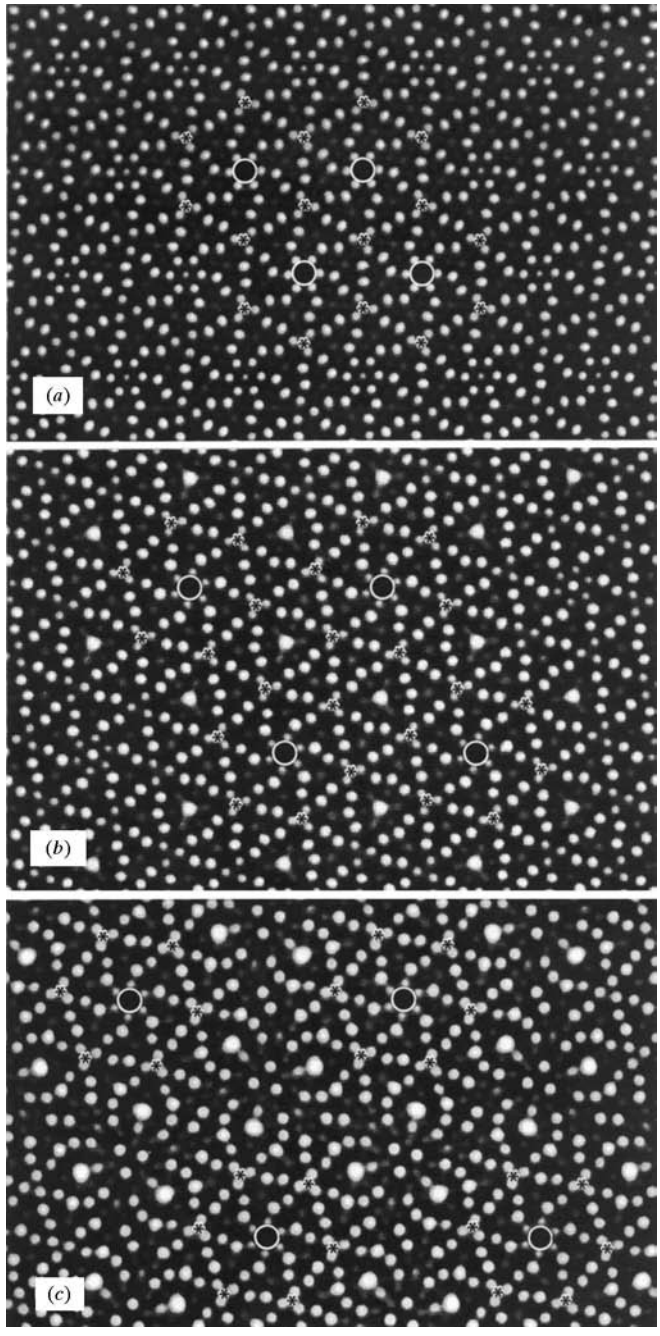

Figure 1
[001] High-resolution electron microscopic images of the hexagonal phases κ-$Al_{76}Cr_{18}Ni_6$, λ-$Al_{4.32}Mn$ and ν-$Al_{80.61}Cr_{10.71}Fe_{8.68}$, showing the same hexagon of image points marked with asterisks at its corners around a lattice point (large solid circle): (*a*) simulated image of κ [calculated from Marsh (1998)], a = 17.674 Å, hexagons are in direct contact; (*b*) simulated image of λ [calculated from Kreiner & Franzen (1997)], a = 28.382 Å, hexagons are separated; (*c*) experimental image of ν, a = 40.687 Å, hexagons are widely separated.

[1] Supplementary data for this paper are available from the IUCr electronic archives (Reference: ZH0020). Services for accessing these data are described at the back of the journal.

Table 2
Occupancies of two special sites.

Atom	κ	λ	ν
#	1Al	0.85 Al, 0.15 Mn	0.52 Al, 0.48 TM
§	1TM	0.60 Al	0.53 Al, 0.47 TM

Fig. 2(*a*) shows a projected (001) layer block of the κ phase whereas Fig. 2(*b*) is that of the λ phase, again calculated from the data given by Marsh (1998) and Kreiner & Franzen (1997), respectively. These (001) layer blocks consist of three layers PFP^m, F being a flat layer at $z = 0.25$, whereas P ($z = 0.04$–0.15) and P^m ($z = 0.35$–0.46) are a pair of puckered layers in mirror reflection across the F layer. The atoms in the F layer are connected by a thin line, and the atoms in the P and P^m layers are superimposed on each other. There are altogether six layers in a c period and the atom sites in the other three layers, $(PFP^m)'$, can be obtained from the PFP^m layers by a 6_3 operation. The hexagonal atomic motif, marked with asterisks around a lattice point in Fig. 2, corresponds to the hexagon of image points also marked with asterisks in Fig. 1. These hexagonal motifs are in direct contact in Fig. 2(*a*), as in Fig. 1(*a*), but are separated in Fig. 2(*b*). It is to be noted that the similarity in atomic distribution around a lattice point in κ and λ phases can be extended beyond this hexagonal atomic motif to a larger truncated triangular area outlined by a thick line in Fig. 2. These areas are overlapped in the κ phase (for clarity, only the overlapping in one direction is shown), whereas they are slightly separated in the λ phase. The atomic distributions within this area in these two phases are almost identical except that (i) the few atomic sites marked # and § around a lattice point are differently occupied (data of the ν phase determined in the present study are also included), see Table 2; (ii) there are more TM atoms, marked ‡ in Fig. 2(*a*), in the puckered layer of the κ phase, but these sites are unoccupied in the λ structure. A similar case can be found in the related Al_5Co_2 and β-Al_9Mn_3Si structures, and the corresponding atomic sites are occupied in the former (Bradley & Cheng, 1938) but vacant in the latter (Robinson, 1952). As pointed out earlier by Franzen & Kreiner (1993) and Kreiner & Franzen (1997), all the TM atoms within the outlined area in the λ phase are icosahedrally coordinated, although these

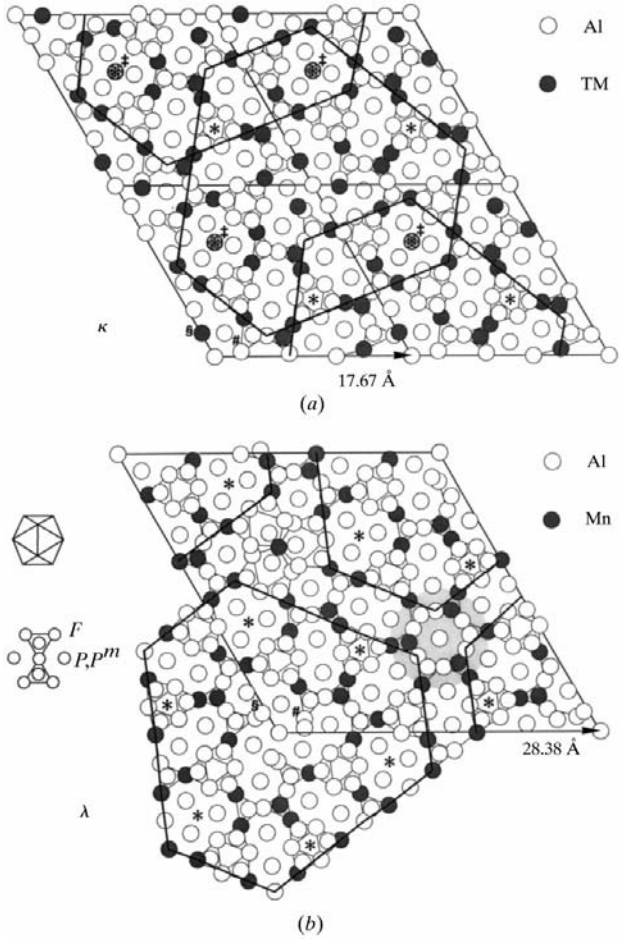

Figure 2
[001] Projection of atoms in a PFP^m layer block, where the atoms in the flat layer F are connected by a thin line and the atoms are in superimposition on each other in the puckered layers P and P^m in mirror reflection across F: (*a*) κ [calculated from Marsh (1998)] and (*b*) λ [calculated from Kreiner & Franzen (1997)]. Asterisks indicate the hexagons corresponding to those in Figs. 1(*a*) and 1(*b*), respectively. Thick lines highlight the almost identical complex icosahedral clusters in these two phases. These clusters are overlapped in κ but slightly separated from each other in λ.

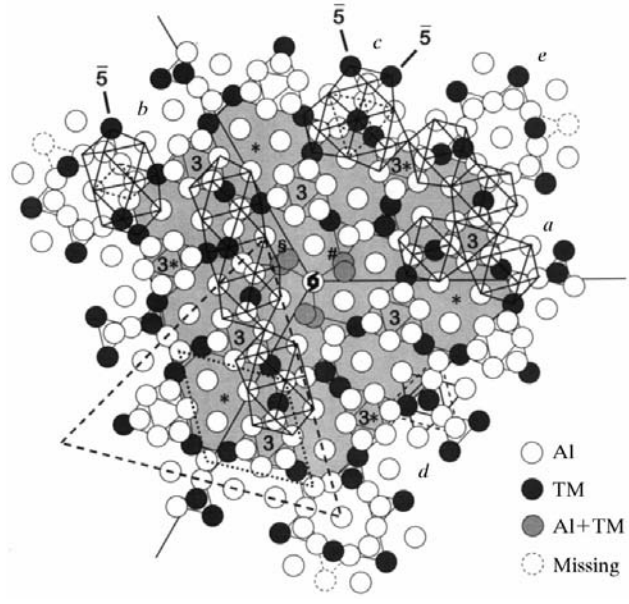

Figure 3
The experimentally determined complex icosahedral cluster in the PFP^m layer block of the ν phase (shaded area) in which the atoms in the flat layer F are connected. Icosahedral spikes are growing outwards from this complex icosahedral cluster to form more icosahedral bonds. Thick dashed lines mark a corresponding layer block in the hexagonal μ-Al_4Mn, whereas the dotted lines indicate that in the hexagonal β-Al_9Mn_3Si. (*a*) Three vertex-sharing icosahedra [called I3 cluster by Kreiner & Franzen (1995) and denoted '3' here]; (*b*) two interpenetrated icosahedra along their $\bar{5}$ axis; (*c*) three interpenetrated icosahedra; (*d*) the atoms at the central part of three interpenetrated icosahedra form an icosahedron with its $\bar{3}$ axis parallel to the c axis; (*e*) incomplete ring of four interpenetrated icosahedra [compare with the six icosahedra ring in the shaded area in Fig. 2(*b*)].

icosahedra are all slightly deformed (see also an enlarged view of this area in the ν phase shown in Fig. 3). On the left of the [001] projection of the λ phase in Fig. 2(*b*), an icosahedron with its twofold axis normal to the paper is shown either in a wire diagram (upper) or as open circles (lower). In the former case, eight triangles of the icosahedron can be seen in this top view (there are four more triangles projected as straight lines). In the latter case, Kreiner & Franzen (1995) used connecting lines of two inverted triangles to show the atoms on the *F* layer, and four atoms each on the *P* and P^m layers. Most of the icosahedral connection in the complex icosahedral cluster in Figs. 2 and 3 can thus be recognized.

3.2. X-ray diffraction

Both complex icosahedral clusters in the κ and λ phases have been used as the atomic configuration at the origin of the unit cell of the ν phase for structural expansion and the same structural model with a relatively low *R* value was generated by direct methods using the program *SHELXS*97 (Sheldrick, 1997*a*). This model was then refined by full-matrix least-squares methods using the program *SHELXL*97 (Sheldrick, 1997*b*). Final $R = 0.075$, goodness of fit $S = 1.085$, 3854 reflections with $F_o > 4\sigma(F_o)$, and 474 variables ($R1 = 0.1250$ and $wR2 = 0.2068$ for all 5453 reflections). The maximum and minimum values in the final difference Fourier map were +1.61 and −1.30 e Å^{-3}, respectively. Fe and Cr atoms have not been distinguished completely. Except three unique sites occupied by Fe atoms and nine by Cr atoms, other TM sites were supposed to be occupied by 50%Cr + 50%Fe and the averaged scattering factors were used. Final atomic coordinates and isotropic thermal parameters are listed together with occupancy values in Table 3 and the former is shown schematically in Fig. 4. All TM sites and those Al sites with icosahedral coordination are marked with asterisks in Table 3 and also marked in Fig. 4.

There are 31 TM sites and 100 Al sites in one asymmetric unit. Some sites are statistically shared by Al and TM atoms,

Table 3
Atomic sites, coordinates, isotropic thermal parameters and occupancy factors for ν-$Al_{80.61}Cr_{10.71}Fe_{8.68}$.

Asterisks indicate icosahedral sites. Atom site sign Al: Al predominant; TM, Cr or Fe: TM, Cr or Fe predominant; M: mixed Al and TM.

Atom	Site	*x*	*y*	*z*	U_{iso}	Occupancy
Al1	2(*a*)	0	0	0.2500	0.003 (10)	0.47Al + 0.03TM
Al2	4(*e*)	0	0	0.1099 (18)	0.001 (4)	0.50
Al3	4(*f*)	0.6667	0.3333	0.0426 (9)	0.005 (2)	1.00
Cr4*	6(*h*)	0.03193 (15)	0.90723 (14)	0.2500	0.0037 (11)	1.00
Cr5*	6(*h*)	0.18049 (15)	0.85053 (15)	0.2500	0.0050 (12)	1.00
Cr6*	6(*h*)	0.33670 (14)	0.02076 (15)	0.2500	0.0061 (12)	1.00
Cr7*	6(*h*)	0.59667 (14)	0.15519 (14)	0.2500	0.0042 (12)	1.00
Cr8*	6(*h*)	0.75065 (15)	0.09767 (15)	0.2500	0.0084 (12)	1.00
Cr9*	6(*h*)	0.84274 (15)	0.21868 (14)	0.2500	0.0049 (13)	1.00
Cr10*	6(*h*)	0.94010 (16)	0.18129 (15)	0.2500	0.0060 (12)	1.00
Cr11*	6(*h*)	0.99335 (14)	0.15933 (14)	0.2500	0.0028 (11)	1.00
TM12*	6(*h*)	0.03669 (15)	0.75047 (15)	0.2500	0.0089 (12)	1.00
TM13*	6(*h*)	0.06812 (15)	0.66065 (15)	0.2500	0.0081 (12)	1.00
TM14*	6(*h*)	0.12878 (15)	0.87186 (15)	0.2500	0.0090 (12)	1.00
TM15	6(*h*)	0.14507 (19)	0.71979 (18)	0.2500	0.010 (2)	0.60TM + 0.40Al
TM16	6(*h*)	0.27105 (17)	0.52623 (17)	0.2500	0.008 (2)	0.62TM + 0.38Al
TM17	6(*h*)	0.27959 (16)	0.81464 (16)	0.2500	0.0100 (12)	1.00
TM18*	6(*h*)	0.31882 (15)	0.94934 (15)	0.2500	0.0093 (12)	1.00
TM19*	6(*h*)	0.37904 (16)	0.77809 (17)	0.2500	0.010 (2)	0.81TM + 0.19Al
TM20*	6(*h*)	0.46032 (14)	0.05536 (14)	0.2500	0.0080 (11)	1.00
TM21*	6(*h*)	0.49307 (14)	0.96621 (14)	0.2500	0.0056 (12)	1.00
TM22*	6(*h*)	0.62837 (15)	0.06518 (15)	0.2500	0.0078 (11)	1.00
TM23*	6(*h*)	0.80862 (14)	0.30749 (14)	0.2500	0.0089 (12)	1.00
TM24*	6(*h*)	0.84853 (14)	0.06002 (14)	0.2500	0.0083 (11)	1.00
M25	6(*h*)	0.9647 (2)	0.0358 (2)	0.2500	0.019 (3)	0.48TM + 0.52Al
Al26	6(*h*)	0.0567 (3)	0.5951 (3)	0.2500	0.007 (2)	1.00
Al27	6(*h*)	0.0722 (3)	0.8798 (3)	0.2500	0.011 (2)	1.00
Al28*	6(*h*)	0.0881 (3)	0.7318 (3)	0.2500	0.004 (2)	1.00
Al29	6(*h*)	0.0962 (3)	0.9616 (3)	0.2500	0.024 (3)	1.00
Al30*	6(*h*)	0.1081 (3)	0.8020 (3)	0.2500	0.002 (2)	1.00
Al31	6(*h*)	0.1538 (3)	0.9409 (3)	0.2500	0.015 (3)	1.00
Al32	6(*h*)	0.2147 (5)	0.7549 (5)	0.2500	0.040 (6)	0.84
Al33	6(*h*)	0.2234 (3)	0.8253 (3)	0.2500	0.012 (2)	1.00
Al34	6(*h*)	0.2475 (3)	0.9053 (3)	0.2500	0.007 (2)	1.00
Al35	6(*h*)	0.3039 (3)	0.8842 (3)	0.2500	0.013 (2)	1.00
Al36	6(*h*)	0.3120 (3)	0.7186 (3)	0.2500	0.0043 (19)	1.00
Al37*	6(*h*)	0.3896 (3)	0.0029 (3)	0.2500	0.010 (2)	1.00
Al38	6(*h*)	0.4117 (3)	0.9089 (3)	0.2500	0.020 (4)	0.83Al + 0.17TM
Al39*	6(*h*)	0.4298 (3)	0.7613 (3)	0.2500	0.027 (4)	0.76Al + 0.24TM
Al40*	6(*h*)	0.4412 (3)	0.9843 (3)	0.2500	0.006 (2)	1.00
Al41	6(*h*)	0.4606 (3)	0.8424 (3)	0.2500	0.016 (2)	1.00
Al42	6(*h*)	0.4614 (4)	0.6740 (4)	0.2500	0.037 (4)	1.00
Al43	6(*h*)	0.5321 (3)	0.0969 (3)	0.2500	0.011 (2)	1.00
Al44	6(*h*)	0.5459 (3)	0.1706 (3)	0.2500	0.011 (2)	1.00
Al45	6(*h*)	0.5583 (3)	0.0238 (3)	0.2500	0.005 (2)	1.00
Al46	6(*h*)	0.6207 (3)	0.0018 (3)	0.2500	0.005 (2)	1.00
Al47*	6(*h*)	0.6476 (3)	0.1361 (3)	0.2500	0.012 (2)	1.00
Al48	6(*h*)	0.6680 (3)	0.2091 (3)	0.2500	0.013 (2)	1.00
Al49*	6(*h*)	0.6991 (3)	0.1178 (3)	0.2500	0.010 (3)	0.87Al + 0.13TM
Al50	6(*h*)	0.7159 (3)	0.3462 (3)	0.2500	0.010 (2)	1.00
Al51	6(*h*)	0.7259 (3)	0.0290 (3)	0.2500	0.011 (2)	1.00
Al52	6(*h*)	0.7355 (3)	0.2554 (3)	0.2500	0.020 (3)	1.00
Al53*	6(*h*)	0.7708 (3)	0.1682 (3)	0.2500	0.014 (3)	0.92Al + 0.08TM
Al54	6(*h*)	0.7828 (3)	0.0071 (3)	0.2500	0.008 (2)	1.00
Al55*	6(*h*)	0.7909 (3)	0.2372 (3)	0.2500	0.011 (2)	1.00
Al56	6(*h*)	0.8048 (3)	0.0856 (3)	0.2500	0.011 (2)	1.00
Al57	6(*h*)	0.8804 (3)	0.3484 (3)	0.2500	0.004 (2)	1.00
Al58	6(*h*)	0.8834 (3)	0.1897 (3)	0.2500	0.007 (2)	1.00
Al59*	6(*h*)	0.9010 (3)	0.0398 (3)	0.2500	0.013 (2)	1.00
Al60	6(*h*)	0.9088 (3)	0.2744 (3)	0.2500	0.011 (2)	1.00
Al61*	6(*h*)	0.9207 (3)	0.1107 (3)	0.2500	0.010 (2)	1.00
Al62	6(*h*)	0.9656 (3)	0.2497 (3)	0.2500	0.006 (2)	1.00
Fe63	12(*i*)	0.14240 (8)	0.61874 (8)	0.0633 (3)	0.0044 (6)	1.00
Fe64	12(*i*)	0.70289 (9)	0.23518 (8)	0.0733 (3)	0.0087 (7)	1.00
Fe65	12(*i*)	0.73475 (8)	0.35062 (8)	0.0534 (2)	0.0051 (6)	1.00
Cr66*	12(*i*)	0.73951 (9)	0.12994 (9)	0.0766 (3)	0.0031 (7)	1.00
TM67*	12(*i*)	0.07945 (9)	0.76160 (9)	0.0748 (3)	0.0077 (7)	1.00

Table 3 (continued)

Atom	Site	x	y	z	U_{iso}	Occupancy
TM68	12(*i*)	0.39138 (10)	0.89074 (10)	0.0530 (3)	0.0060 (11)	0.81TM + 0.19Al
TM69*	12(*i*)	0.42939 (9)	0.01312 (9)	0.0754 (3)	0.0060 (7)	1.00
TM70*	12(*i*)	0.89035 (9)	0.07075 (9)	0.0751 (3)	0.0075 (8)	1.00
M71	12(*i*)	0.98087 (16)	0.04531 (16)	0.0464 (5)	0.0241 (18)	0.47TM + 0.53Al
Al72	12(*i*)	0.0028 (2)	0.8395 (2)	0.1365 (6)	0.0115 (17)	1.00
Al73	12(*i*)	0.00492 (19)	0.2216 (2)	0.1341 (6)	0.0087 (16)	1.00
Al74	12(*i*)	0.00535 (18)	0.74239 (18)	0.0569 (6)	0.0090 (15)	1.00
Al75	12(*i*)	0.02462 (19)	0.16719 (19)	0.0693 (6)	0.0133 (17)	1.00
Al76	12(*i*)	0.02517 (19)	0.68767 (19)	0.1361 (6)	0.0063 (15)	1.00
Al77	12(*i*)	0.0326 (2)	0.9590 (2)	0.1458 (7)	0.0240 (19)	1.00
Al78	12(*i*)	0.04435 (19)	0.63116 (19)	0.0694 (6)	0.0107 (15)	1.00
Al79	12(*i*)	0.05941 (19)	0.9144 (2)	0.0651 (6)	0.0141 (16)	1.00
Al80	12(*i*)	0.0613 (2)	0.8159 (2)	0.1347 (6)	0.0081 (16)	1.00
Al81	12(*i*)	0.09837 (18)	0.70722 (19)	0.0614 (6)	0.0086 (14)	1.00
Al82	12(*i*)	0.1180 (2)	0.6554 (2)	0.1371 (6)	0.0120 (16)	1.00
Al83	12(*i*)	0.11879 (18)	0.89340 (18)	0.0705 (5)	0.0066 (14)	1.00
Al84	12(*i*)	0.13639 (19)	0.83721 (19)	0.0647 (6)	0.0108 (15)	1.00
Al85	12(*i*)	0.1531 (2)	0.78225 (19)	0.1377 (7)	0.0116 (17)	1.00
Al86	12(*i*)	0.16097 (19)	0.56140 (19)	0.1375 (6)	0.0075 (15)	1.00
Al87	12(*i*)	0.1641 (2)	0.4319 (2)	0.0717 (7)	0.0201 (18)	1.00
Al88	12(*i*)	0.17214 (14)	0.73356 (14)	0.0587 (5)	0.0114 (17)	0.71Al + 0.29TM
Al89	12(*i*)	0.1939 (2)	0.9138 (2)	0.1328 (6)	0.0068 (15)	1.00
Al90	12(*i*)	0.1959 (2)	0.6898 (2)	0.1335 (6)	0.0108 (16)	1.00
Al91	12(*i*)	0.2077 (2)	0.6312 (2)	0.0557 (6)	0.0165 (16)	1.00
Al92	12(*i*)	0.21199 (18)	0.85803 (18)	0.0677 (6)	0.0083 (14)	1.00
Al93	12(*i*)	0.27552 (19)	0.97233 (19)	0.1327 (6)	0.0081 (16)	1.00
Al94	12(*i*)	0.29474 (18)	0.91707 (18)	0.0670 (6)	0.0088 (14)	1.00
Al95	12(*i*)	0.33166 (18)	0.04641 (17)	0.0702 (6)	0.0073 (14)	1.00
Al96	12(*i*)	0.3370 (2)	0.8499 (2)	0.1370 (7)	0.018 (3)	0.87
Al97	12(*i*)	0.35193 (18)	0.99159 (18)	0.0641 (6)	0.0082 (14)	1.00
Al98	12(*i*)	0.3655 (2)	0.7136 (2)	0.1311 (6)	0.0130 (17)	1.00
Al99	12(*i*)	0.3731 (2)	0.9386 (2)	0.1358 (5)	0.0099 (16)	1.00
Al100	12(*i*)	0.40795 (19)	0.06524 (19)	0.1359 (6)	0.0062 (15)	1.00
Al101	12(*i*)	0.41792 (17)	0.65273 (17)	0.0537 (6)	0.0070 (14)	1.00
Al102	12(*i*)	0.43661 (18)	0.72931 (18)	0.0562 (6)	0.0102 (15)	1.00
Al103	12(*i*)	0.44743 (18)	0.95708 (18)	0.0581 (7)	0.0115 (16)	1.00
Al104	12(*i*)	0.4674 (2)	0.9068 (2)	0.1327 (6)	0.0113 (16)	1.00
Al105	12(*i*)	0.48329 (18)	0.08619 (18)	0.0552 (6)	0.0077 (14)	1.00
Al106	12(*i*)	0.4982 (3)	0.7256 (3)	0.0922 (8)	0.022 (3)	0.84
Al107	12(*i*)	0.5017 (2)	0.03015 (19)	0.1359 (6)	0.0063 (15)	1.00
Al108	12(*i*)	0.52460 (18)	0.97830 (18)	0.0694 (6)	0.0074 (14)	1.00
Al109	12(*i*)	0.56637 (18)	0.13897 (18)	0.0605 (6)	0.0101 (15)	1.00
Al110	12(*i*)	0.5870 (2)	0.0899 (2)	0.1357 (6)	0.0136 (17)	1.00
Al111	12(*i*)	0.60568 (19)	0.03463 (19)	0.0692 (6)	0.0121 (15)	1.00
Al112	12(*i*)	0.61537 (19)	0.21344 (19)	0.1374 (6)	0.0088 (16)	1.00
Al113	12(*i*)	0.64393 (19)	0.16902 (18)	0.0623 (6)	0.0116 (15)	1.00
Al114	12(*i*)	0.66306 (19)	0.10882 (19)	0.0598 (6)	0.0115 (15)	1.00
Al115	12(*i*)	0.68393 (19)	0.28295 (19)	0.1195 (5)	0.0069 (14)	1.00
Al116	12(*i*)	0.6846 (2)	0.0569 (2)	0.1367 (6)	0.0092 (15)	1.00
Al117	12(*i*)	0.7194 (2)	0.1849 (2)	0.1306 (6)	0.0075 (16)	1.00
Al118	12(*i*)	0.75885 (18)	0.07369 (18)	0.0572 (6)	0.0105 (15)	1.00
Al119	12(*i*)	0.76254 (18)	0.31908 (18)	0.1378 (6)	0.0076 (15)	1.00
Al120	12(*i*)	0.77458 (17)	0.26177 (17)	0.0657 (6)	0.0062 (14)	1.00
Al121	12(*i*)	0.79724 (19)	0.20399 (19)	0.0641 (6)	0.0100 (15)	1.00
Al122	12(*i*)	0.8140 (2)	0.1486 (2)	0.1390 (6)	0.0109 (17)	1.00
Al123	12(*i*)	0.81693 (19)	0.05171 (19)	0.0574 (6)	0.0122 (15)	1.00
Al124	12(*i*)	0.83502 (19)	0.33443 (19)	0.0656 (6)	0.0114 (15)	1.00
Al125	12(*i*)	0.8548 (2)	0.2817 (2)	0.1369 (6)	0.0111 (16)	1.00
Al126	12(*i*)	0.8731 (2)	0.1260 (2)	0.1361 (6)	0.0095 (16)	1.00
Al127	12(*i*)	0.87326 (17)	0.22510 (18)	0.0701 (6)	0.0067 (14)	1.00
Al128	12(*i*)	0.90992 (19)	0.01769 (19)	0.0560 (6)	0.0125 (15)	1.00
Al129	12(*i*)	0.93007 (19)	0.20256 (19)	0.0696 (6)	0.0108 (15)	1.00
Al130	12(*i*)	0.94878 (19)	0.14683 (19)	0.0656 (6)	0.0099 (15)	1.00
Al131	12(*i*)	0.9664 (2)	0.0919 (2)	0.1375 (6)	0.0152 (17)	1.00

especially sites 25 and 71 which are about equally occupied by Al and TM atoms (denoted by M in Table 3 and shown as shaded circles in Fig. 4). Thanks to the partial occupancy, the total number of Al atoms is thus 954.88 and those of Cr and Fe atoms are 126.84 and 102.84, respectively, leading to the formula $Al_{80.61}Cr_{10.71}Fe_{8.68}$.

The number of neighbors (N) and interatomic distances (<3 Å) for all Al and TM atoms has been calculated. The distribution of atoms along the 6_3 axis at the origin shows an abnormal short distance, such as 1.76 Å between Al1 and Al2 [marked 1 and 2 separately in Figs. 4(*a*) and 4(*b*)]. This implies that these two positions cannot be simultaneously occupied or each has a 50% occupation. With this exception the interatomic distance ranges are TM—TM 2.606–2.838, TM—Al 2.203–2.949 and Al—Al 2.432–2.999 Å. The bond length between TM16 and Al39 is the shortest, 2.203 Å, but is still comparable with Co—Al, 2.24 Å, in orthorhombic $Al_{13}Co_4$ (Grin *et al.*, 1994). Abnormal short contacts between a TM atom and some of the surrounding Al atoms, interpreted as a result of the transfer of electrons between them, were considered to be characteristic of the structures of the Al-rich Al–TM compounds (Taylor, 1954). As can be seen in Table 3, only about 70% of TM atoms are icosahedrally coordinated in comparison with about 98% for the λ phases. Obviously, the TM atoms 15, 16 and 17 in Fig. 4(*a*) do not have icosahedral coordination, as do the TM/Fe atoms 63–65 and 68 in Fig. 4(*b*).

Among the 100 independent Al atom sites in an asymmetric unit, one has CN8, 12 have CN9, 14 have CN10, 29 have CN11 and 44 have CN12 coordination. About a quarter of the Al atoms are also icosahedrally coordinated, such as 28, 30, 37 and 40 in some of the icosahedral chains in Fig. 4(*a*).

4. Description and discussion

4.1. Complex icosahedral cluster

As in the related hexagonal κ and λ phases, the structure of the ν phase also consists of six layers stacked along the c axis. The atoms in the flat layer F (z = 0.25) are shown as large circles connected by thin lines, whereas those in the puckered layers P (z = 0.04–0.15) and P^m (z = 0.35–0.46) are shown as small circles in Fig. 4(*a*). Thanks to the mirror reflection across the F

layer, a compound layer block of PFP^m results. Referring to the atomic configuration shown on the left-hand side of Fig. 2(*b*), the icosahedra in the layer block PFP^m can easily be identified. The complex icosahedral cluster around the hexagonal lattice point is outlined by a thick line. Between these complex icosahedral clusters there are also many TM/Cr atoms in icosahedral coordination, as the TM/Cr atoms 7, 13 and 20–23 in Fig. 4(*a*). Fig. 4(*b*) shows the atoms in the FP^mP' layer block, in which the connecting lines linking the atoms in the flat layer *F* are retained.

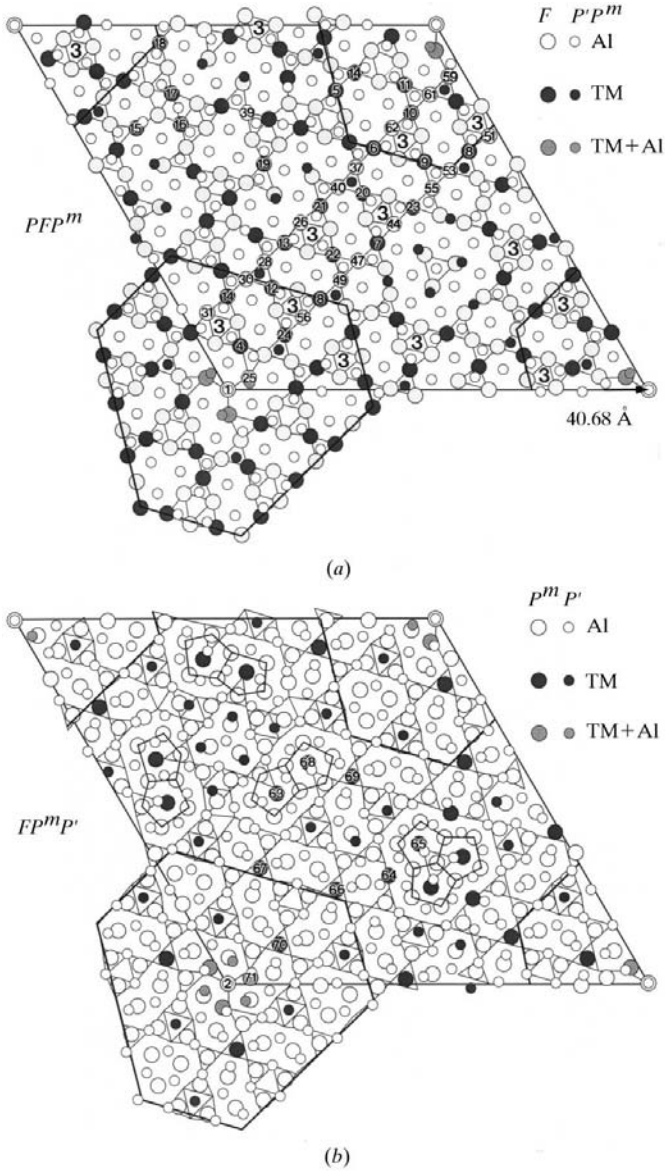

Figure 4
Atomic distribution in (*a*) the PFP^m layer block and (*b*) the FP^mP' layer block of the ν phase, in which the complex icosahedral cluster is outlined by a thick line. The three vertex-sharing icosahedra, denoted by '3' in (*a*), form further interpenetrated icosahedral chains in the intermediate region between these complex icosahedral clusters. In addition, there are also many icosahedra with their $\bar{3}$ axis parallel to the *c* axis [centered about TM/Cr atoms 66, 67, 69 *etc.* in Fig. 4(*b*)] forming icosahedral bonds between the PFP^m and $(PFP^m)'$ layer blocks. However, pentagonal prisms with both ends capped by transition-metal atoms [highlighted in Fig. 4(*b*)] also exist in this region.

Obviously, the atom sites in the complex icosahedral cluster in the ν phase, except those few marked with # and § around a lattice point in Fig. 3 which are mixed occupied and drawn in shaded circles, are basically the same as those in the κ and λ phases shown in Fig. 2. In order to show the icosahedral coordination in the complex icosahedral cluster, the atoms in both the flat and puckered layers are shown in Fig. 3. The atoms in the flat layer *F* are connected, whereas those in the *P* and P^m layers, in mirror reflection with respect to *F*, are superimposed on each other. The shaded truncated triangular area shows the complex icosahedral cluster used for structural expansion and some more atoms surrounding this cluster are included to show the extension of icosahedral coordination outwards. Several typical cases of interconnection of icosahedra are highlighted by a thick line in Fig. 3, as follows.

(*a*) Three icosahedra with their twofold axes parallel to the *c* axis share vertices with each other forming an empty triangle in the flat layer. The atoms at the vertices of the inverted triangles in the *P* and P^m layers (see also Fig. 4*a*) form a pair of face-sharing octahedra. This interconnection of icosahedra has been discussed earlier by Edström & Westman (1971) in $RuZn_6$, by Kripjakevich (1977) in the hexagonal β-Al_9Mn_3Si, and by Wen *et al.* (1992) in connection with the μ-Al_4Cr phases. In a comprehensive discussion of the icosahedral packing, Kreiner & Franzen (1995) called the three vertex-sharing icosahedra an I3 cluster. For clarity, such I3 clusters in Fig. 3 are marked '3' only. It can be seen in Fig. 3 that, except at the origin, these I3 clusters cover almost evenly the entire truncated triangular area.

(*b*) Two icosahedra interpenetrate each other along their pseudo $\bar{5}$ axis and they share a common pentagon capped on both sides, namely, a pentagonal biprism (broken lines). In fact, this chain of two interpenetrated icosahedra can be expanded downwards to an I3 cluster forming a chain of three interpenetrated icosahedra. To its right side there are another two chains of four and two interpenetrated icosahedra, respectively. It is of interest to note that such a chain ends at an I3 cluster forming a pentagonal prism between the end members of two neighboring chains. In Fig. 4(*a*) such pentagonal prisms are centered at Al26, 31, 44, 51, 56 and 62. Therefore, the chain of four interpenetrated icosahedra can also be visualized as a series of four pentagonal antiprisms capped with two halves of a pentagonal prism. It is of interest to note that the $\bar{5}$ axes are parallel to three sides of the truncated triangular area, rather than the $\langle 100 \rangle$ directions as in μ-Al_4Mn (Shoemaker *et al.*, 1989).

(*c*) Three mutually interpenetrated or fused icosahedra whose centers form a small triangle (drawn in broken lines) in the flat layer with an atom in the *P* layer at the triangle center. Two $\bar{5}$ axes parallel to two sides of this truncated triangle are indicated while the third is parallel to the third side. The icosahedron of some of the I3 clusters (such as that with the TM12 atom at its center in Fig. 4*a*) is also connected to two other icosahedra forming a cluster of three interpenetrated icosahedra (around the TM67 atom in Fig. 4*b*). Li *et al.* (1997) called such a set of three three-interpenetrated icosahedra associated with an I3 cluster an ico-9 cluster. Such a case also

exists in the structure of β-Al_9Mn_3Si (Kripjakevich, 1977) and μ-Al_4Mn (Shoemaker *et al.*, 1989).

(*d*) The central part of these three-interpenetrated icosahedra at *c* itself is an icosahedron with its $\bar{3}$ axis parallel to the *c* direction. For clarity, this is shown separately in a symmetrically related position at *d* in Fig. 3. However, only the three triangles in the *F* and P^m layers are shown here (the six Al atoms in the P^m layer belong in fact to two sets of three Al atoms at slightly different *z* levels), since the fourth triangle is in the P' layer. On the other hand, the four alternately oriented triangles of an icosahedra in the layer block FP^mP' projected along its $\bar{3}$ axis can be seen more clearly in Fig. 4(*b*), in which the TM/Cr atoms 66, 67 and 70 are located at the centers of these icosahedra. Since the flat layer *F* is a mirror, there is another icosahedron below *F* in the $P^{m\prime}PF$ layer block. It shares a triangular face with the icosahedron above it, thus forming an icosahedral chain of two face-sharing icosahedra in this direction. This serves as an icosahedral bond between the PFP^m and $(PFP^m)'$ icosahedral layer blocks in the *c* direction.

(*e*) In the shaded area in Fig. 2(*b*) there is a ring of six interpenetrated icosahedra sharing in common a pair of atoms at the center (located respectively on the *P* and P^m layers) around $\frac{2}{3}$, $\frac{1}{3}$, $\frac{1}{4}$. This hexagonal configuration was shown in $Mg_{51}Zn_{20}$ by Higashi *et al.* (1981), in μ-Al_4Mn by Shoemaker *et al.* (1989) and in detail in λ-Al_4Mn by Kreiner & Franzen (1995, 1997). However, owing to a missing atom shown as dotted circles in Fig. 3, such a ring of six interpenetrated icosahedra at *e* is incomplete, and there are only four interpenetrated icosahedra.

4.2. Relationship to κ and λ

It becomes clear from the above discussion that the truncated triangular cluster is the main building block of the structures of κ, λ and ν phases. Since this truncated triangle is in a skew position with respect to the hexagonal $\langle 100 \rangle$ axes, varying slightly in these three phases, there is no mirror or glide plane parallel to the *c* axis. Or in other words, their space group is $P6_3/m$ but not $P6_3/mmc$ as in μ-Al_4Mn and β-Al_9Mn_3Si. It can be seen in Figs. 2 and 3 that the angle between the long side of the truncated triangle and the *a* axis increases from 22° in κ to 38° in λ and 45° in ν. This agrees with the fact that the strong diffraction spot in the [001] electron diffraction pattern of the κ, λ and ν phases occurs at about 22, 38 and 45°, respectively, from the reciprocal [100]* axis [see Fig. 7(*a*) in Li *et al.* (1997), Fig. 5(*a*) in Bendersky (1987*b*) and Fig. 1(*a*) in Sui *et al.* (1999)].

In the κ structure these complex icosahedral clusters outlined in Fig. 2(*a*) are overlapping with each other and consequently almost all TM atoms, except those marked § and ‡, are icosahedrally coordinated. In the λ structure these complex icosahedral clusters are so closely positioned (Fig. 2*b*) that the icosahedral spikes shown in Fig. 3 of two neighboring complex icosahedral clusters superimpose on each other forming icosahedral bonds between them, including the six interpenetrated icosahedra at $\frac{2}{3}$, $\frac{1}{3}$, $\frac{1}{4}$. Therefore, 102 of the 104 Mn atoms in a λ unit cell are icosahedrally coordinated, and the other two Mn atoms at the centers of trigonal prisms at $\frac{1}{3}$, $\frac{2}{3}$, $\frac{1}{4}$ and $\frac{2}{3}$, $\frac{1}{3}$, $\frac{3}{4}$ have a coordination number of 9 (Kreiner & Franzen, 1997). This also occurs in μ-Al_4Mn (Shoemaker *et al.*, 1989). On the other hand, these complex icosahedral clusters in the ν structure are widely separated (Fig. 4). Nevertheless, some icosahedral chains between two neighboring complex icosahedral clusters do exist, as shown by the I3 clusters '3' in the intermediate area between them in Fig. 4(*a*). Some of the TM atoms in Fig. 4(*b*) also have icosahedral coordination, such as TM69, with a $\bar{3}$ axis along the *c* axis. However, pentagonal prisms capped with TM/Fe atoms also occur in pairs or in a group of three sharing a prismatic face (outlined in Fig. 4*b*) in this area. In the latter case the central atoms of these three face-sharing pentagonal prisms form a pair of face-capped trigonal prisms with a CN9 Al atom at the center (Fig. 4*a*). The coordination number of these TM atoms is 10–11. This is the reason why the icosahedral coordination of the TM atoms in the ν phase is relatively low (about 70%) in comparison with that in the κ and λ structures consisting of similar complex icosahedral clusters. As discussed by Li *et al.* (1998), each unit cell of the orthorhombic ε-Al_4Cr phase consists of, among other things, two incomplete unit cells of the hexagonal κ phase and there are pairs of pentagonal prisms capped with TM atoms similar to those outlined in Fig. 4(*b*) between two κ unit cells. The atomic configurations of the top-capped trigonal and pentagonal prisms have been illustrated in Fig. 19 of Kreiner & Franzen (1997), such as those polyhedra centered around atoms 1 and 8, respectively.

From the above discussion it is clear that the hexagonal κ, λ and ν phases have the same type of $PFP^m(PFP^m)'$ layer structure and consequently have about the same *c* parameters (~12.4–12.6 Å) and almost the same complex icosahedral cluster. Therefore, we can take advantage of the known structures of the κ and λ phases to solve the structure of the ν phase by X-ray diffraction, thanks to the same local characteristics around a lattice point in the [001] HREM images of these three phases. This shows the benefit of a combination of HREM and X-ray diffraction in the study of intermetallic structures.

4.3. Relationship to μ and β

Since the hexagonal μ-Al_4Mn and λ-Al_4Mn are structurally closely related (Kreiner & Franzen, 1995, 1997), it is expected that the structures of the ν and μ phases should also be related. In Fig. 3 a PFP^m slab of one half of the (001) plane-cell of μ-Al_4Mn [see Fig. 1(*d*) of Shoemaker *et al.* (1989)] is outlined by a dashed line, although the set of six interpenetrated icosahedra at its lattice points in Fig. 3 is incomplete. Owing to a missing atom shown by the dotted circle at *e*, only four interpenetrated icosahedra exist, whereas there are six interpenetrated icosahedra in the μ-Al_4Mn structure. In the hexagonal μ-Al_4Mn the pseudo-icosahedral symmetry is propagated along the $\langle 100 \rangle$ axial directions as interpenetrated icosahedral chains (Shoemaker *et al.*, 1989; Shoemaker, 1993).

However, owing to the skew position of the complicated icosahedral cluster with respect to the ⟨100⟩ directions in ν, the pseudo-icosahedral chains in it are deviated about 45° from the hexagonal ⟨100⟩ axes. It is known that the unit cell of the β-Al_9Mn_3Si exists within the μ-Al_4Mn unit cell (Shoemaker *et al.*, 1989), therefore it should also exist in the ν phase (outlined by a dotted line in Fig. 3). Le Lann & Shoemaker (1993) and Shoemaker (1994) have discussed the structural relationship between μ-Al_4Mn and the icosahedral/decagonal quasicrystal and a similar relation might also exist between the ν phase and a quasicrystal.

4.4. Relationship to other hexagonal layer structures

Recently another family of hexagonal layer structures, with about the same c values, 8.6–8.87 Å, but with the parameter a in approximate 3:5:7 ratios, have been found in Zn_6Mg_3RE (RE: rare earth metals) alloys (Table 1). They are called S, M and L phases, respectively, by Abe *et al.* (1999) and μ_3, μ_5 and μ_7 phases, respectively, by Sugiyama *et al.* (1998, 1999). The structure of S-$Zn_{65.22}Mg_{27.92}Y_{6.86}$ ($P6_3/mmc$, a = 14.579 Å, c = 8.687 Å) has been solved by single-crystal X-ray diffraction (Takakura *et al.*, 1998). In the mean time, the structures of μ_3-$Zn_{65.2}Mg_{28.3}Sm_{6.5}$ ($P6_3/mmc$, a = 14.619, c = 8.708 Å) and μ_7-$Zn_{64.8}Mg_{24.1}Sm_{11.1}$ ($P6_3/mmc$, a = 33.565, c = 8.873 Å) were shown to consist of three and seven icosahedra, respectively, in an a period (Sugiyama *et al.*, 1998, 1999). They correspond to the S and L phases of Abe *et al.* (1999) and are in fact superstructures of the C-14 Friauf–Laves phase $MgZn_2$ (Friauf, 1927; $P6_3/mmc$, a = 5.16, c = 8.50 Å). In $MgZn_2$ there is only one icosahedron in an a period and the threefold axis of this icosahedron is parallel to the c axis. On the other hand, in the Zn_6Mg_3RE superstructures only the icosahedra at the lattice points are so oriented (although compressed in c), whereas all other icosahedra are distorted and have one of their twofold axes approximately parallel to the c axis. Sugiyama *et al.* (1999) have discussed the hypothetical μ_5 superstructure with five icosahedra along its a axis. Such a structure with an intermediate a parameter (a = 23.5, c = 8.6 Å) was in fact found in a Zn_6Mg_3Sm alloy by electron diffraction and was called the M phase by Abe *et al.* (1999). All these phases co-exist with an icosahedral quasicrystal, which was found to be a stable quasicrystalline phase in Zn–Mg–RE alloys (Takakura *et al.*, 1998). The reversible quasicrystal–crystal transformation in these alloys has also been discussed recently (Abe & Tsai, 1999).

In contrast to the κ, λ and ν layer structures with a layer-stacking sequence of $PFP^m(PFP^m)'$ and a c period of about 12.4 Å, the S, M and L Zn–Mg–RE layer structures have two flat and two puckered layers in a c period of 8.6−8.87 Å. The two F layers are again located at z = 0.25 and 0.75 and the two P layers are related either by a mirror reflection across F or by a 6_3 screw operation. In this context the layer stacking sequence in the S, M and L Zn–Mg–RE structures is closely related to the β-Al_9Mn_3Si structure. Moreover, they all have a higher space-group symmetry ($P6_3/mmc$) than the κ, λ and ν structures ($P6_3/m$).

This work was generously supported by the Chinese Academy of Sciences and by the National Natural Science Foundation of China. The authors are grateful to Dr K. Sun for supplying the $Al_{12}Cr_2Fe$ ingot in which the single crystal of the ν phase used in the present study was found. Professor Q. Lu, China University of Geosciences (Wuhan), and Professor Q. J. Wu, Fujian Research Institute for Structure of Matters of the Chinese Academy of Sciences, kindly allowed us to use their X-ray apparatus for data collection. Drs X. Z. Li, J. K. Liang, Z. S. Ma, N. C. Shi, Clara B. Shoemaker and K. Urban are thanked for helpful discussions and constructive comments.

References

Abe, E., Takakura, H., Singh, A. & Tsai, A. P. (1999). *J. Alloys Compd*, **283**, 169–172.
Abe, E. & Tsai, A. P. (1999). *Phys. Rev. Lett.* **83**, 753–756.
Audier, M. & Guyot, P. (1986). *J. Phys. (Suppl.)* **47**, C3-405–C3-414.
Bendersky, L. (1987*a*). *J. Microsc.* **146**, 303–312.
Bendersky, L. (1987*b*). *Mater. Sci. Forum*, **22/24**, 151–161.
Bradley, A. J. & Cheng, C. S. (1938). *Z. Kristallogr.* **99**, 480–487.
Daams, J. L. C., Villars, P. & van Vucht, J. H. N. (1991). *Atlas of Crystal Structure Types for Intermetallic Phases.* Materials Park, Ohio: Materials Information Society.
Dubois, M.-J., Janot, J. & de Boissieu, M. (1988). *Quasicrystalline Materials*, edited by M.-J. Dubois & C. Janot, pp. 97–106. Singapore: World Scientific.
Edström, V.-A. & Westman, S. (1971). *Chem. Scr.* **1**, 137–143.
Elser, V. & Henley, L. (1985). *Phys. Rev. Lett.* **55**, 2883–2886.
Franzen, H. F. & Kreiner, G. (1993). *J. Alloys Compd*, **202**, L21–L24.
Friauf, J. B. (1927). *Phys. Rev.* **29**, 34–40.
Grin, J., Burkhardt, U., Ellner, M. & Peters, K. (1994). *J. Alloys Compd*, **206**, 243–247.
Hårsta, A. & Runqvist, S. (1987). *J. Solid State Chem.* **70**, 210–218.
Higashi, I., Shiotani, N., Uda, M., Mizoguchi, T. & Katoh, H. (1981). *J. Solid State Chem.* **36**, 225–233.
Hovmöller, S. (1992). *Ultramicroscopy*, **41**, 121–135.
Kreiner, G. & Franzen, H. F. (1995). *J. Alloys Compd*, **221**, 15–36.
Kreiner, G. & Franzen, H. F. (1997). *J. Alloys Compd*, **261**, 83–104.
Kripjakevich, P. I. (1977). *Structural Types of Intermetallic Compounds.* Moscow: Nauk. (In Russian.)
Le Lann, A. & Shoemaker, C. B. (1993). *J. Non-Cryst. Solids*, **153/154**, 654–657.
Li, X. Z., Hiraga, K. & Yamamoto, A. (1997). *Philos. Mag. A*, **76**, 657–666.
Li, X. Z. & Kuo, K. H. (1988). *Philos. Mag. Lett.* **58**, 167–171.
Li, X. Z., Sui, H. X., Kuo, K. H., Sugiyama, K. & Hiraga, K. (1998). *J. Alloys Compd*, **264**, L9–L12.
Liao, X. Z., Sui, H. X. & Kuo, K. H. (1998). *Philos. Mag. A*, **78**, 143–156.
Marsh, R. E. (1998). *Acta Cryst.* B**54**, 925–926.
Robinson, K. (1952). *Acta Cryst.* **5**, 397–403.
Samson, S. (1987). *Mater. Sci. Forum*, **22/24**, 83–102.
Sato, A., Yamamoto, A., Li, X. Z., Hiraga, K., Haibach, T. & Steurer, W. (1997). *Acta Cryst.* C**53**, 1531–1533.
Sheldrick, G. M. (1997*a*). *SHELXS97. Program for the Solution of Crystal Structure.* University of Göttingen, Germany.
Sheldrick, G. M. (1997*b*). *SHELXL97. Program for the Refinement of Crystal Structure.* University of Göttingen, Germany.
Shoemaker, C. B. (1993). *Philos. Mag. B*, **67**, 869–881.
Shoemaker, C. B. (1994). *Mater. Sci. Forum*, **150/151**, 191–198.

Shoemaker, C. B., Keszler, D. A. & Shoemaker, D. P. (1989). *Acta Cryst.* B**45**, 13–20.
Sugiyama, K., Yasuda, K., Ohsuna, T. & Hiraga, K. (1998). *Z. Kristallogr.* **213**, 537–543.
Sugiyama, K., Yasuda, K., Ohsuna, T. & Hiraga, K. (1999). *J. Alloys Compd.* **285**, 172–178.
Sui, H. X., Li, X. Z. & Kuo, K. H. (1999). *Philos. Mag. Lett.* **79**, 181–185.
Sui, H. X., Liao, X. Z., Kuo, K. H., Zou, X. D. & Hovmöller, S. (1997). *Acta Cryst.* B**53**, 587–595.
Takakura, H., Sato, A., Yamamoto, A. & Tsai, A. P. (1998). *Philos. Mag. Lett.* **78**, 263–270.
Taylor, M. A. (1959). *Acta Cryst.* **12**, 393–396.
Taylor, W. H. (1954). *Acta Metall.* **2**, 684–695.
Wen, K. Y., Chen, Y. L. & Kuo, K. H. (1992). *Metall. Trans. A*, **23**, 2437–2445.